Chiral Resolution of a Mn 3+ Spin Crossover Complex

Vibe Jakobsen, Luke O'Brien, Ghenadie Novitchi, Helge Müller-Bunz, Anne-Laure Barra, Grace Morgan

Chiral Resolution of a Mn(III) Spin Crossover Complex

Vibe B. Jakobsen,[a] Luke O'Brien,[a]Ghenadie Novitchi,[b] Helge Müller-Bunz,[a] Anne-Laure Barra,[b] and Grace G. Morgan*[a]

[a] V. B. Jakobsen, L. O'Brien, Dr. H. Müller-Bunz, Dr. G. G. Morgan
School of Chemistry
University College Dublin
Science Centre Belfield, Dublin 4, Ireland
E-mail: grace.morgan@ucd.ie
Homepage: https://people.ucd.ie/grace.morgan
[b] Dr. G. Novitchi, Dr. A.-L. Barra
Laboratoire National des Champs Magnétiques Intenses (LNCMI)
Centre National de la Recherche Scientifique (CNRS)
25 Rue des Martyrs, BP 166, 38042 Grenoble Cedex 9, France

Abstract: Enantiopure Δ and Λ forms of the spin crossover Mn^{3+} chelate complex $[Mn(5\text{-}OCF_3\text{-}sal_2(323))]^+$ were prepared by cocrystallization with the (R,R) and (S,S) forms of the chiral spiroborate anion bis-[1,1'-binaphthyl-2,2'-diolato]boron. The absolute structures of the enantiomers were established by X-ray crystallography at 100 K and at 293 K. The enantiomeric purity of the Δ and Λ forms in acetonitrile solution was confirmed by circular dichroism spectroscopy in the UV-vis range. Both enantiomers show a gradual and incomplete S = 1 ↔ S = 2 thermal spin crossover in the solid state but persist mainly in the spin triplet form between 3-200 K and retain a high percentage of spin triplet character at room temperature.

Introduction

Chirality and magnetism are intimately linked, both in molecule based and solid state magnets. In the solid state this is demonstrated by the many different forms of chiral magnetic order that exist, including the helicoidal arrangements of electron spins in magnetic domain walls,[1] the inherent chirality of quantum solitons[2] or the spin textures in skyrmions.[3] Molecular chirality is also important in magnetism, particularly in spintronic applications where the aim is to induce spin polarization. Naaman and Waldeck have recently reported that ordered films of diamagnetic chiral organic molecules, such as DNA, can act as spin filters towards a current of unpolarized mobile electrons in an effect they term Chiral-Induced Spin Selectivity (CISS).[4] The CISS effect is modelled as arising due to spin-orbit coupling of an electron spin passing through the helical electric field of the film of chiral molecules. This generates a magnetic field that splits the spin orientations of the mobile electron, producing a spin polarization that can be detected when the electron arrives at the surface. The spin filtering efficiency is closely related to helical pitch and length and the effect has also been implicated in catalytic electron transfer reactions on surfaces of photocatalysts which have been appended with chiral molecules.[5] The CISS effect demonstrates that a mobile electron spin can sense the environment of the chiral diamagnetic medium through which it moves. It is also of interest therefore to study the effect of directly implanting a spin in a chiral molecule, where it may then acquire a phase depending on the degree of magnetic anisotropy and spin orbit coupling. Such an effect has indeed been detected by magnetochiral dichroism[6] in magnetically ordered molecules,[7] and in enantiopure paramagnetic rare earth clusters[8] and in helicoidal chains of magnetically anisotropic transition metal ions such as Co^{2+}.[9]

Synthetic approaches to prepare enantiopure coordination compounds include use of a chiral ligand, (chirality@ligand) or use of an achiral chelating ligand which twists around the coordinated ion in clockwise or anticlockwise fashion thereby conferring chirality at the metal centre (chirality@metal). Although this latter type of chirality is very prevalent in coordination compounds, the majority of chelate complexes crystallize as racemates in centrosymmetric spacegroups. Resolution of the racemates may however be possible by cocrystallization with charge-balancing chiral counterions, (chirality@counterion), although crystallization of a mixture of diastereoisomers is also a possibility.

A chiral paramagnet designed to incorporate an internal switching mechanism may have potential for gated spintronic applications, *i.e.* one where the spin acquires a phase from the molecular chirality, and in addition some property of the spin such as magnitude or direction, can also be switched, thereby allowing a gated modulation. Spin crossover (SCO) compounds, which are capable of switching between low spin (LS) and high spin (HS) states,[10] may be suitable candidates for this role. SCO complexes are typically hexacoordinate d^4-d^7 first row transition metal complexes and switching is usually thermally activated, although non-thermal routes[10b] have also been reported including use of light, pressure, magnetic or electric fields, or chemical modification *e.g.* changing pH.[11] To date both the chirality@ligand[12] and combined chirality@metal/chirality@counterion[13] approaches have been used to successfully generate enantiopure iron SCO complexes. For example use of chiral ligands, such as optically active Schiff base amines[12f] or macrocyclic ligands with asymmetric substituents[12a-e] yield enantiopure SCO compounds. Use of the chirality@metal approach can also be used to yield a broad range of 1D-3D chiral polymeric structures showing SCO behaviour.[14] Spontaneous resolution of SCO enantiomers has also been reported from achiral starting materials where the crystal packing accounts for the homochiral crystallisation of complexes.[14e, 15] Aside from Fe^{2+}/Fe^{3+}, SCO is also possible in octahedral Co^{2+} and Mn^{3+} complexes, although it is less common.[16] In Mn3+ the switching is between the S = 1 intermediate spin (IS) triplet and the S = 2 HS quintet states, and it has been realised in a small number of coordination spheres by different perturbations including pressure,[17] temperature,[18] and magnetic and/or electric fields.[19] Switching between the spin triplet and spin quintet forms allows injection of a significant distortion into the lattice due to the Jahn-Teller effect in the spin quintet form, and this has particular relevance for ferroelectric or piezoelectric applications where significant atomic displacements are required. As such applications necessitate crystallization in noncentrosymmetric lattices, we were interested to prepare enantiopure Mn^{3+} SCO complexes. We have reported several examples of thermally induced spin state switching in Mn^{3+} using a simple Schiff base hexadentate ligand type which we term R-sal_2(323).[18b-h, 20] Complexes prepared with this ligand type are inherently chiral as the $N_4O_2^{2-}$ hexadentate Schiff-base ligand has chirogenic amine nitrogen atoms, Scheme 1. However, the complexes crystallise predominantly either as racemates in centrosymmetric space groups or as mechanical mixtures of chiral conglomerates of Δ and Λ isomers. Here, we introduce for the first time two chiral spiroborate counterions (S,S)-bis-[1,1'-binaphthyl-2,2'-diolato]boron, (S,S)-X^- and (R,R)-bis-[1,1'-binaphthyl-2,2'-diolato]boron, (R,R)-X^- for the Mn^{3+} complex cation, $[Mn(5\text{-}OCF_3\text{-}sal_2(323))]^+$, abbreviated $[MnL]^+$ for clarity. Only 15 structures containing the spiroborate anion are reported in the CCDC crystallographic database (ConQuest version 2.0.0)[21] and these are predominantly organic salts.[22] The magnetic properties and chirality of the complexes were characterized with SQUID magnetometry and circular dichroism respectively.

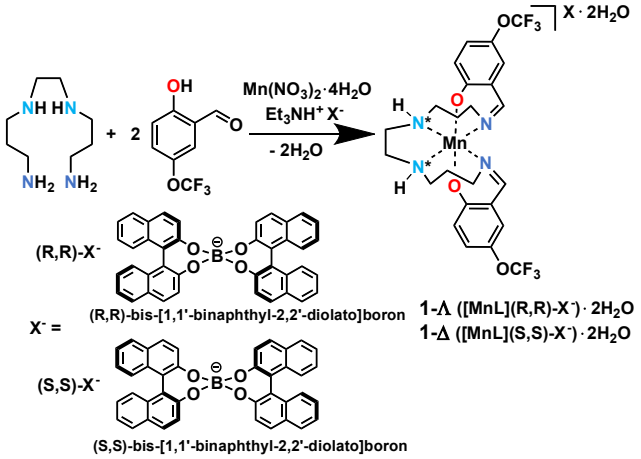

Scheme 1. Synthesis of **1-Λ** [Mn(5-OCF_3-sal$_2$(323))]((R,R)-X)·2H_2O and**1-Δ** [Mn(5-OCF_3-sal$_2$(323))]((S,S)-X)·2H_2O and with the "*" highlighting the chirogenic amine nitrogen atom.

Results and Discussion

Synthesis: The chiral anions were readily synthesized as triethylammonium salts according to literature procedures.[23] Equimolar amounts of triethylammonium (R,R)-bis-[1,1'-binaphthyl-2,2'-diolato]boron, $[Et_3NH]^+$[(R,R)-X]$^-$ (or the $[Et_3NH]^+$[(S,S)-X]$^-$ enantiomer) and Mn$(NO_3)_2$·4H_2O were mixed in EtOH/CH_3CN and added to a solution containing the ligand (5-OCF_3-sal$_2$(323), H_2L, prepared by Schiff-base condensation of 2-hydroxy-5-(trifluoromethoxy)benzaldehyde and 1,2-bis(3-aminopropylamino)ethane in a 1:1 mixture of EtOH:CH_3CN. The Mn^{3+} complex crystallised as enantiopure crystalline batches of Δ-[MnL]((S,S)-X)·solvent, **1-Δ** or Λ-[MnL]((R,R)-X)·solvent, **1-Λ** where solvent is a mixture of H_2O and CH_3CN in the crystallised material (**1-Λ/Δ·CH_3CN·4H_2O**) depending on temperature. In attempts with other R-sal$_2$(323) ligands combinations of various diastereoisomers were obtained but the complexes recovered with 5-OCF_3-sal$_2$(323) were enantiopure as described below. At 100 K, the crystal structure contains acetonitrile and at 293 K, the acetonitrile molecule has evaporated from the crystal structure (*vide infra*).The number of H_2O molecules, n, varies from crystal to crystal, Table S1. The bulk sample contains two water molecules which is estimated from elemental analysis (**1-Λ/Δ·2H_2O**). When referring to the complexes, **1-Λ** and **1-Δ** will be used for crystal structures and **1-Λ·2H_2O** and **1-Δ·2H_2O** for dry bulk samples.

X-ray Crystallography: Complexes 1-Λ and1-Δ crystallise in the chiral non-centrosymmetric tetragonal space group I422 and contain the $[MnL]^+$ cation, the spiroborate anions (S,S)-X$^-$ or (R,R)-X$^-$,and acetonitrile and water solvates, Figure 1 and Figure S1-S4. Only 80 crystal structures are reported to crystallise in this highly symmetric tetragonal I422 space group in the CCDC crystallographic database (ConQuest version 2.0.0)[21] which renders the I422 space group rather rare. 1-Λ and 1-Δ both contain one CH_3CN solvent molecule which was located at 100 K and is disordered over two positions both lying on a 4-fold rotation axis. The remaining water solvate molecules were severely disordered and treated using the Platon Squeeze software tool[24] to compensate for the remaining unassigned electron density in the structures. Data sets were collected at 100 K (below the spin crossover) and at 293 K (toward the end of the incomplete crossover) for each enantiomer (*vide infra*).

In each complex, the absolute structure was determined unambiguously from the diffraction data. The main features of the structure are the same in each case. The d^4 Mn(III) ion in the cation is bound to a hexadentate *trans*-N_4O_2-ligand and geometry around the Mn(III) centre is best described as approximately octahedral. There is no indication of a geometric Jahn-Teller effect: at 100 K the Mn-N_{imine} and Mn-N_{amine} bonds are similar to those of other related Mn(III) S = 1 complexes, Table 1.[18f]

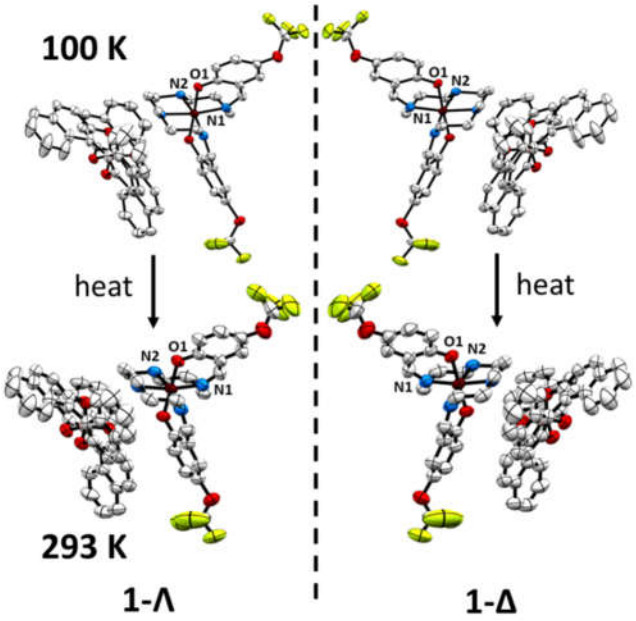

Figure 1. Perspective views of the two enantiomeric complexes 1-Λ and 1-Δ at 100 K and 293 K respectively shown with 50% atomic probability distributions for ellipsoids with acetonitrile solvent molecules and hydrogen atoms are omitted for clarity.

At 293 K, an increase in bond length for both Mn-$N_{imine}$and Mn-N_{amine} is observed, and the values of CShM[25], ΣMn and Φ[26], which measures the degree of octahedral distortion in relation to spin-state changes, are also higher, as expected, for the 293 K structure than for the 100 K structures.

Table 1. Selected bond lengths (Å) and structural parameters of **1-Λ** and **1-Δ** at 100 K and 293 K.

	Selected Bond distances (Å)			
Mn donor	**1-Λ (100 K)**	**1-Λ (293 K)**	**1-Δ (100 K)**	**1-Δ (293 K)**
Mn–O_{phen}	1.8792(13)	1.8808(15)	1.8809(16)	1.8805(17)
Mn–N_{imine}	2.0072(17)	2.040(2)	2.008(2)	2.034(2)
Mn–N_{amine}	2.0421(17)	2.076(2)	2.042(2)	2.067(2)
CShM[a]	0.461	0.677	0.446	0.602
ΣMn[b]	41.37	48.9	40.39	45.77
Φ[c]	97.34	118.11	96.24	111.66

[a]CShM: continuous shape measure relative to ideal octahedron; [b]Σ Mn: the sum of the deviation from 90° of the 12 cis-angles of the MnN_4O_2 octahedron,[c]Φ: the sum of the deviation from 60° of the 24 trigonal angles of the projection of the MnN_4O_2 octahedron onto the trigonal faces.

The spiroborate anion has approximately tetrahedral geometry at the boron atom and shows no unusual bond lengths or angles, Table S2. Both the Mn(III) cation and the boron atom of the anion sit on 2-fold rotation axes so that the asymmetric unit contains half of the cation and half of the anion.

The amine donors of the cation are H-bonded to oxygen atoms of the spiroborate anions, Figure 2 and Figures S5-S8. This results in a spiral chain of alternating cations and anions running about a 2-fold screw axis parallel to the

c axis. In addition, weak interactions between two Mn(III) cations CH····OCF_3 and weak interactions between the Mn(III) cation and the spiroborate counterion CH····OBO_3 and CH····F_3CO are found at 100 K for **1-Δ**, Figure S9. At 293 K, the CH····F_3CO interaction between the Mn(III) cation and the spiroborate anion can no longer be considered as a weak interaction and this may contribute to the onset of the spin state switching. The differences in the intermolecular distances for CH····F_3CO at 100 K and 293 K for **1-Δ** and **1-Λ** are 0.21 Å and 0.168 Å respectively.

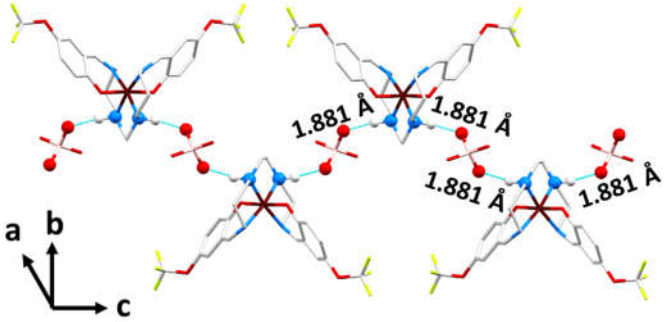

Figure 2. View of 1D hydrogen bonding chain of complex **1-Λ** at 100 K shown with capped sticks; boron oxygen atoms and amine nitrogen atoms involved in hydrogen bonding are represented with ball-and-stick figures. Phenyl rings on spiroborate anion and non-heteroatoms hydrogen atoms omitted for clarity.

A small increase in intermolecular distance of the H-bonding is observed at 293 K compared to 100 K for both 1-Λ and 1-Δ, Table S3. This cooperative effect may facilitate loss loss of the acetonitrile molecule on warming (Figures S11-S12), thereby assisting the spin state change which requires a higher volume. There are no intermolecular interactions between neighbouring chains. A void space calculation using contact surface maps of each **1-Λ** and **1-Δ** complex at 100 K and 293 K shows an increase in total void space of 2.5 % going from 100 K to 293 K, Figure S13-S14 and Table S4.

For crystalline materials, chirality may be attributed to either themolecule itself, the asymmetric unit and its ovarall packing, or even external crystal faces (hemihedral crystallization).[27] Molecular chirality in the Mn(III) complex cations arises from the spatial arrangement of non-equivalent atom groups surrounding the chirogenic nitrogen amine atoms (R,R or S,S), Figure 3a and Figure S15, on the hexadentate ligand creating a twist aroundthe metal centre in a Δ (clockwise) and Λ (anticlockwise) mode, Figure S16.

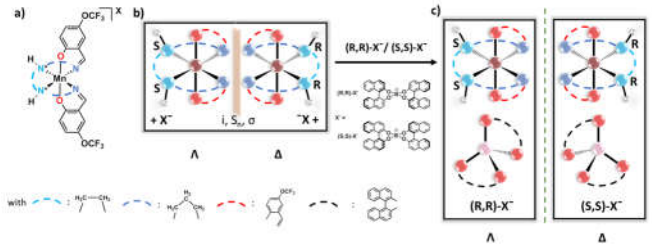

Figure 3. Schematic representation of a) the molecular structure of the Mn(III) complex cation with the "*" highlighting the chirogenic amine nitrogen atoms, b) ball-stick figures showing co-crystallisation of enantiomeric Λ and Δ Mn(III) complex cations related by a mirror of rotoinversion operations or glide reflections generating racemic crystals when any X^- anion is used, c) the resolution of the enantiomeric Mn(III) complex cations, Λ and Δ, with the chiral spiroborate anions (R,R)-X^- and (S,S)-X^- respectively creating enantiopure crystals.

The Δ and Λ molecules can exist in a racemic mixture which allows them to either crystallize as a racemate with both enantiomers present in the unit cell which are related by pure rotoinversion operations ($\bar{1}$, m, $\bar{3}$, $\bar{4}$, $\bar{6}$) or glide reflection, Figure 3b, or in a Sohncke space group where each single crystal is optically active but with an overall racemic bulk composition. Moreover, the aforementioned hydrogen bonding of the Mn(III) complex cation and the spiroborate anion is another source of chirality as they form a helical arrangement with the Λ enantiomer showing a left-handed helix, P and the Δ enantiomer showing a right-handed helix, M, Figure 4.[28]

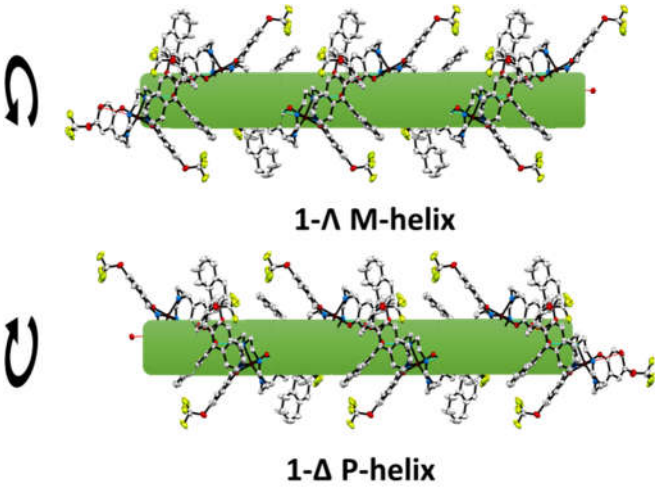

Figure 4. Helical arrangement of the **1-Λ** (top) and **1-Δ** (bottom) complex viewed along the b-axis which includes the Mn(III) complex cation and (R,R)/(S,S)-X^- anion around a rod showing the anti-clockwise (M-helix, top) and clockwise (P-helix, bottom) arrangement of cation and anion.

Circular Dichroism: The circular dichroism (CD) spectrum of the chiral spiroborate salt, $[Et_3NH]^+[(S,S)\text{-}X]^-$ (Figure 5 inset, green dashed line) exhibits a positive Cotton effect in the UV region at λ_{max} = 256.5 nm with another positive Cotton effect at λ_{max}= 227 nm respectively, Figure 5 (inset). Moreover, $[Et_3NH]^+[(S,S)\text{-}X]^-$ exhibits a negative differential absorption in the UV region at λ = 206 nm, 223.5, nm and 252.5 nm with positive differential absorptions at λ = 238 nm and 267 nm respectively, Figure 5. The spiroborate salt $[Et_3NH]^+[(R,R)\text{-}X]^-$ (blue dashed line) shows Cotton effects of the opposite sign at the same wavelengths. To our knowledge, this is the first time CD spectra of the spiroborate salts, $[Et_3NH]^+[(R,R)\text{-}X]^-$ and $[Et_3NH]^+[(S,S)\text{-}X]^-$ have been recorded. For the Mn(III) complexes **1-Λ·2H₂O** (black line) and **1-Δ·2H₂O** (red line) Cotton effects in the UV region fit, as expected, with that of the chiral spiroborate salts with the same handedness.

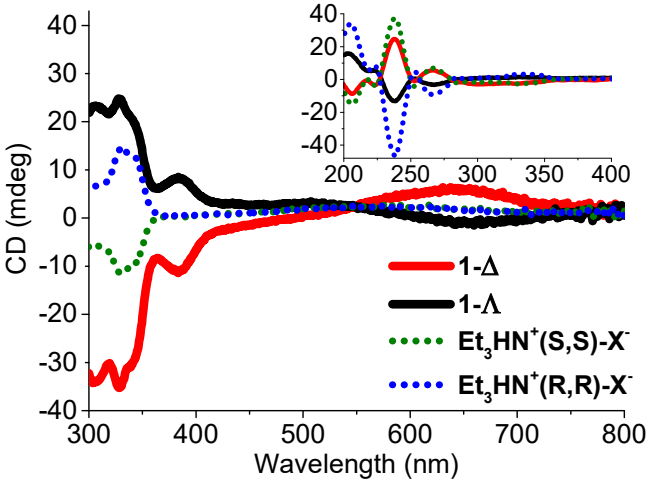

Figure 5. Circular dichroism spectra of chiral spiroborate anion salts, $[Et_3NH]^+[(R,R)\text{-}X]^-$ (blue dashed line), $[Et_3NH]^+[(S,S)\text{-}X]^-$ (green dashed line) and complexes **1-Δ** (red line) and **1-Λ**(black line) showing predominantly the features of the enantiopure Mn(III) complex cations in the visible region and enantiopure spiroborate anion in the UV region (inset).

Spectra in the visible region for both the counterion salts and the Mn(III) complexes were collected on more concentrated solutions between 300-800 nm. In this region the spectrum of the chiral spiroborate salt [Et3NH]+[(S,S)-X]$^-$ shows a negative differential absorption at λ = 329 nm and that of [Et3NH]+[(R,R)-X]$^-$ shows a positive differential absorption at λ = 330 nm, Figure 5.

The CD spectrum of **1-Λ·2H$_2$O** exhibits a positive differential absorption at λ = 303.5 nm, 328 nm, 383.5 nm and 644.5 nm, while **1-Δ·2H$_2$O** shows a differential absorption effect of the opposite sign at the same wavelengths. **1-Λ·2H$_2$O** exhibits a negative Cotton effect in the UV region at λ_{max}= 550 nm and **1-Δ·2H$_2$O**show a positive Cotton effect of at the same wavelengths. Hence, the CD spectra recorded in solution confirm the optical activity and enantiomeric nature of **1-Λ·2H$_2$O** and **1-Δ·2H$_2$O**. The CD spectra in the visible region was investigated again after 6 days on the same solutions as the initial CD spectra were measured on (Figure S17) and confirms that the Mn(III) complex cation does not racemise fast in solution as might have been expected since asymmetric tertiary amines are not substitutionally inert and can readily undergo pyramidal inversion. There is however, a small decrease in the differential absorptions for both**1-Λ·2H$_2$O**and **1-Δ·2H$_2$O**at λ = 303.5 nm, 383.5 nm and 644.5 nm which are the differential absorptions associated with the Mn(III) complexes. So it cannot be ruled out that over a longer period of time, the enantiopure Mn(III) complexes will racemise.

Magnetic Properties: Magnetic measurements of complexes **1-Λ** and **1-Δ** were recorded using a Quantum Design SQUID magnetometer (MPMS-XL) between 2-300 K in cooling and warming modes at 0.1 T, Figure 6. The microcrystalline samples of **1-Λ** and **1-Δ** were filtered from their mother solution immediately before the measurements to avoid loss of the volatile CH_3CN solvents, which potentially could lead to decay of the crystals if left out of their mother liquor for a long period of time. Despite this, some differences in the $\chi_M T$ values over the measured range were apparent and these were attributed to different degrees of solvation. However the main outcome of the magnetic study was to establish that both enantiomers show a gradual thermal SCO.

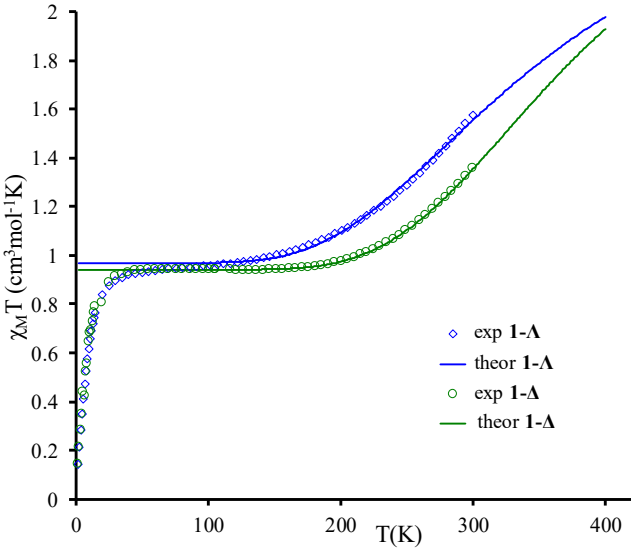

Figure 6. Plots of $\chi_M T$ versus T for complexes **1-Λ** (blue curve) and **1-Δ**(green curve)between 2–300 K. The solid lines correspond to the best fit of the experimental data.

The expected $\chi_M T$ values for the quintet and triplet spin states of Mn(III) are 3 and 1 cm^3 K mol^{-1} respectively (assuming g=2), and plots of $\chi_M T$ versus T, Figure 6, indicate that complex **1-Λ** and **1-Δ** remain at a value of 1 cm^3 K mol^{-1} up to around 200 K above which the $\chi_M T$ value starts to increase, indicating some thermal population of the HS state. The thermal population of the HS state reaches a maximum for the **1-Λ** and **1-Δ** complex of $\chi_M T$ = 1.6 and 1.4 cm^3 K mol^{-1} respectively. This indicates that approximately 30 % for **1-Λ** and 20 % for **1-Δ** of the total spin is in the HS state at room temperature. These results are comparable to those of similar compounds with the same backbone but with a different substitution on the phenolate ring and choice of anions.[18d, 18f]

In order to estimate the transition temperature and thermodynamic parameters of spin transition the following model has been applied.[29]

$$\chi_M T = \chi_{LS} T + \frac{\chi_{HS} T - \chi_{LS} T}{1 + exp\left[\frac{\Delta H^\circ}{RT} - \frac{\Delta S^\circ}{R}\right]} \qquad \textbf{(1)}$$

Assuming the same g factor for HS and LS species, the best fit of magnetic susceptibility of **1-Λ** and **1-Δ** give values of thermodynamic parameters as indicated in Table 2.

Table 2. Thermodynamic parameters obtained from fit of magnetic data for **1-Λ** and **1-Δ**

	ΔH° kJ/mol	ΔS° J/(mol*K)	$T_{1/2}$ (K)	g_{Mn}	R
1-Λ	13.64(8)	34.9(3)	391(1)	1.976	1.06×10^{-4}
1-Δ	9.2(2)	23.6(1)	388(4)	2.005	4.6×10^{-3}

The values for the change in entropy and enthalpy associated with the gradual spin crossover have been found as ΔH°= 13.64(8)kJ/mol and 9.2(2) kJ/mol and ΔS° = 34.9(3) J/(mol*K) and 23.6(1)J/(mol*K) for **1-Λ** and **1-Δ** respectively. These values are higher than for Mn(III) spin crossover complexes which exhibit a cooperative sharp spin crossover[18e, 30] and to our knowledge no previous examples of calculated thermodynamic values for gradual Mn(III) spin crossover compounds have been elucidated. Thermodynamic properties are usually small for a cooperative S=2 ↔ S=1 SCO system and it is noted here that the transitions for **1-Λ** and **1-Δ**are both very gradual, which indicates a very weak cooperativity in the complexes. As the composition of the bulk crystalline material for **1-Λ** and **1-Δ** has been calculated to contain two H_2O molecules per one Mn(III) complex at 293 K, the variation in spin state for the two enantiomers at 293 K might be related to the change in hydrogen bonding for the two complexes. This in turn could be affected by the amount of CH_3CN trapped in each structure at 100 K and at what given time this is released from the pores of the crystal.

The decline of $\chi_M T$ below 30 K can be attributed to zero-field splitting, as expected for the S = 1 state of the d^4 configuration. This results from spin-orbit coupling and depends on the strength of the ligand-field experienced by the metal ion, but has not been further investigated. For **1-Δ,** a cooling-heating sequence was run at 0.1 T to look for hysteresis, which was not detected, Figure S18. Magnetization curves and χ^{-1} can be found in the SI, Figure S19-S22.

Conclusions

In summary, we have shown that by judicious choice of molecular building blocks, it is possible to design and synthesize Mn^{3+} complexes which exhibit two intrinsic physical properties in one compound: spin crossover and chirality. A

new monovalent chiral anion has been introduced to resolve enantiomeric Mn^{3+} SCO cations thereby allowing modulation of magneto-optical properties. In solution, the enantiomeric Mn^{3+} cations showed no sign of rapid racemisation which allowed us to explore the chirality in further detail for both the complex cations and chiral counteranions using circular dichroism spectroscopy. Future work will include expanding the series of chiral spiroborate anions to Fe^{3+} complexes and other Mn^{3+} complexes by varying the backbone of the ligand and the substituted salicylaldehydes. This work will also focus on attempts to synthesize both chiral and polar crystals which can be used in the preparation of multifunctional SCO materials.

Experimental Section

Materials: All chemicals were purchased from Sigma Aldrich or Fluorochem Ltd. All other reagents were purchased from standard sources and were used as received.

Preparation of chiral anions: The chiral anions triethylammonium (R,R)-bis-[1,1'-binaphthyl-2,2'-diolato]boron and triethylammonium(S,S)-bis-[1,1'-binaphthyl-2,2'-diolato]boron were prepared according to literature procedures.[17] Synthetic characterization can be found in the SI.

Complex 1-Λ·2H_2O:2-hydroxy-5-(trifluoromethoxy)benzaldehyde (41.2mg, 0.2mmol) was diluted in a 1:1 solution of EtOH:CH_3CN (3ml). To this 1,2-bis(3-aminopropylamino)ethane (0.018ml, 0.1mmol) was added. This caused a colour change from colourless to yellow. Triethylammonium (R,R)-bis-[1,1'-binaphthyl-2,2'-diolato]boron (68.1mg, 0.1mmol) was dissolved in a solution of 1:1 EtOH:CH_3CN (3ml). To this a solution of $Mn(NO_3)_2{\cdot}4H_2O$ (25.1mg, 0.1mmol) in 1:1 EtOH:CH_3CN (5 ml) was added. The solution changed from milky white to pink. The two solutions were stirred separately for 2 minutes and then the metal salt solution was added to the ligand solution causing acolour change from yellow to deep red-brown. The solution was gravity filtered and allowed to slowly evaporate solvent at room temperature for 2 days whereupon an ether diffusion was carried out. Dark purple needle crystals suitable for single crystal X-ray diffraction were observedafter 3 days. Yield: 21.9 mg (18%). Elemental analysis calcd.for $C_{64}H_{54}BF_6MnN_4O_{10}$ (found) %: C: 63.04 (63.35), H: 4.47 (4.37), N 4.60 (4.84). IR spectroscopy (FT-ATR diamond anvil) v/cm^{-1}: 3126(w), 3058(w), 2926(w), 2873(w), 1615(w), 1590(m), 1543(m), 1505(m), 1464(m), 1427(m), 1370(m), 1335(m), 1248(s), 1205(s), 1176(s), 1123(m), 1087(m), 1070(m), 1034(m), 987(s), 944(m), 911(m), 875(m), 830(m), 813(s), 744(s), 665(w), 632(m), 573(m), 520(m), 477(m), 446(m), 416(m). ESI-MS (MeCN, pos. mode) calcd (found) m/z = 603.12 (603.92 $[M + H]^+$, 10%). ESI-MS (MeCN, neg. mode) calcd (found) m/z = 579.18 (577.53 $[A]^-$, 40%).

Complex 1-Δ·2H_2O: The procedure for the synthesis of complex **1-Δ·2H_2O** was the same as for complex **1-Λ·2H_2O**but the other spiroborate enantiomer triethylammonium (S,S)-bis-[1,1'-binaphthyl-2,2'-diolato]boron was used instead. A 1 mmol scale of reagents was used instead of 0.1 mmol as described in detail above. Thick long dark purple crystals suitable for single crystal X-ray diffraction were observed after 3 days. Yield: 487.6 mg (42% yield). Elemental analysis calcd.for $C_{64}H_{54}BF_6MnN_4O_{10}$ (found) %: C: 63.04 (63.01), H: 4.47 (4.37), N 4.60 (4.61).IR spectroscopy (FT-ATR diamond anvil) v/cm^{-1}: 3128(w), 3058(w), 2926(w), 2973(w), 1615(m), 1590(m), 1543(m), 1505(m), 1464(m), 1427(m), 1370(m), 1333(m), 1248(s), 1207(s), 1172(s), 1070(m), 987(s), 909(m), 813(s), 744(s), 665(w), 632(m), 573(m), 520(w), 477(w), 446(w).ESI-MS (MeCN, pos. mode) calcd (found) m/z = 603.12 (602.91 $[M + H]^+$, 100%).

Physical Measurements and Instrumentation: IR spectroscopy was recorded using a Bruker ALPHA FT-IR spectrometer attached with a single reflection Platinum-ATR sample module. Mass spectrometry was recorded using a Quattro micro TM LC-MS/MS system. Elemental analysis was conducted on an Exeter Analytical CE 440 elemental analyser. Nuclear magnetic resonance was recorded on a Varian 400 MHz spectrometer with chemical shifts referenced relative to the residual solvent signals.

Single Crystal X-ray Diffraction: Single crystal X-ray diffraction was carried out on suitable single crystals using an Oxford Supernova diffractometer (Oxford Instruments, Oxford, United Kingdom). Datasets were measured using monochromatic Cu-Kα radiation for **1-Λ** and **1-Δ**. The temperature was controlled with an Oxford Cryojet instrument. A complete dataset was collected on 2 separate crystals for the 100 K and 293 K measurement for both **1-Λ** and **1-Δ** enantiomers, assuming that the Friedel pairs are not equivalent as the structures were expected to be chiral. Analytical absorption correction based on the shape of the crystals was performed.[31] All structures were solved by direct methods (SHELXS)[32] and refined by full matrix least-squares on F^2 for all data using SHELXL-2014.[33] All hydrogen atoms were added at calculated positions and refined using a riding model. Their isotropic displacement parameters were fixed to 1.2 times the equivalent one of the parent atom. Anisotropic displacement parameters were used for all non-disordered non-hydrogen atoms. The PLATON SQUEEZE procedure[24] was used to treat regions of disordered solvent which could not be modelled in terms of atomic sites. Crystallographic detailsfor both enantiomers are summarized in Table S1 (SI) and crystallographic data for thestructures reported in this paper have been deposited with the Cambridge Crystallographic DataCentre as supplementary publication numbers CCDC-1916422 (**1-Λ**, 100 K), CCDC-1916424 (**1-Λ**, 293 K), CCDC-1916425 (**1-Δ**, 100 K) and CCDC-1916423 (1-**Δ**, 293 K).

CD Spectroscopy: The CD spectra were recorded on a JASCO J-810 spectrometer. Approximately 10 single crystal of the **1-Λ·H_2O**and **1-Δ·H_2O** complexes were dissolved in 10 ml CH_3CN and the solutions were sonicated for about 5 min. A few drops were added to a quartz cuvette and further diluted with CH_3CN. A few mg of the triethylammonium(R,R)- and (S,S)-bis-[1,1'-binaphthyl-2,2'-diolato]boron salts were dissolved in CH_3CN and one drop was added to a quartz cuvette and further diluted with CH_3CN. Different concentrations of the **1-Λ·H_2O**and **1-Δ·H_2O**complexes and the triethylammonium(R,R)- and (S,S)-bis-[1,1'-binaphthyl-2,2'-diolato]boron salts were used for the UV-area and the visible region of the CD spectra respectively. All CD spectra were recorded with a scan rate of 100nm/min.

Magnetic Measurements: Magnetic measurements were carried out on microcrystalline samples with a Quantum Design SQUID magnetometer (MPMS-XL). Variable-temperature (2–300 K) direct-current magnetic susceptibility was measured under an applied magnetic field of 0.1 T. All data were corrected for the contribution of the sample holder and diamagnetism of the samples estimated from Pascal's constants.

Acknowledgments

We would like to thank Science Foundation Ireland (SFI) for support via an Investigator Project Award (12/IP/1703 to G.G.M). This research was also supported by the Irish Research Council GOIPG/2016/73 fellowship (V.B.J.), and CM1305, Explicit Control over Spin-states in Technology and Biochemistry, (ECOSTBio). We would also like to thank Eckhard Bill and his team at Department Molecular Theory and Spectroscopy, MPI-CEC, Germany for recording preliminary SQUID data on these compounds during a COST action CM1305 sponsored winter-school in December 2016.We gratefully thank Vickie McKee, Dublin City University, Ireland for helping out with crystallography analysis and interpretation.

Keywords: Spin crossover • Manganese(III) • Chirality • Spiroborate chiral anion • Circular dichroism

References

[1] N. A. Spaldin, Magnetic Materials: Fundamentals and Applications, 2nd ed., Cambridge University Press, Cambridge, 2010.

[2] H. -B. Braun, J. Kulda, B. Roessli, D. Visser, K. W. Krämer, H.-U. Güdel, P. Böni, Nat. Phys. 2005, 1, 159-163.

[3] H. -B. Braun, Adv. Phys. 2012, 61, 1-116.

[4] a) B. Göhler, V. Hamelbeck, T. Z. Markus, M. Kettner, G. F. Hanne, Z. Vager, R. Naaman, H. Zacharias, Science 2011, 331, 894; b) R. Naaman, D. H. Waldeck, J. Phys. Chem. Lett. 2012, 3, 2178-2187; c) J. M. Abendroth, D. M. Stemer, B. P. Bloom, P. Roy, R. Naaman, D. H. Waldeck, P. S. Weiss, P. C. Mondal, ACS Nano 2019, 13, 4928-4946.

[5] W. Zhang, W. Gao, X. Zhang, Z. Li, G. Lu, Appl. Surf. Sci. 2018, 434, 643-668.

[6] a) J. Goulon, A. Rogalev, F. Wilhelm, C. Goulon-Ginet, P. Carra, D. Cabaret, C. Brouder, Phys. Rev. Lett. 2002, 88, 237401; b) F. Pop, P. Auban-Senzier, E. Canadell, G. L. J. A. Rikken, N. Avarvari, Nat. Commun. 2014, 5, 3757.

[7] C. Train, R. Gheorghe, V. Krstic, L.-M. Chamoreau, N. S. Ovanesyan, G. L. J. A. Rikken, M. Gruselle, M. Verdaguer, Nat. Mater. 2008, 7, 729.

[8] M. Ceolín, S. Goberna-Ferrón, J. R. Galán-Mascarós, Adv. Mater. 2012, 24, 3120-3123.

[9] R. Sessoli, M.-E. Boulon, A. Caneschi, M. Mannini, L. Poggini, F. Wilhelm, A. Rogalev, Nat. Phys. 2014, 11, 69.

[10] a) O. Kahn, Molecular magnetism, VCH, 1993; b) M. A. Halcrow, Spin-Crossover Materials: Properties and Applications, John Wiley & Sons Ltd, Oxford, UK, 2013.

[11] a) R. Nowak, E. A. Prasetyanto, L. De Cola, B. Bojer, R. Siegel, J. Senker, E. Rössler, B. Weber, Chem. Comm. 2017, 53, 971-974; b) X.-Q. Chen, Y.-D. Cai, W. Jiang, G. Peng, J.-K. Fang, J.-L. Liu, M.-L. Tong, X. Bao, Inorg. Chem. 2019, 58, 999-1002.

[12] a) Q. Wang, S. Venneri, N. Zarrabi, H. Wang, C. Desplanches, J.-F. Létard, T. Seda, M. Pilkington, Dalton Trans. 2015, 44, 6711-6714; b) R. T. Acha, M. Pilkington, CrystEngComm 2015, 17, 8897-8905; c) L.-F. Qin, C.-Y. Pang, W.-K. Han, F.-L. Zhang, L. Tian, Z.-G. Gu, X. Ren, Z. Li, CrystEngComm 2015, 17, 7956-7963; d) D.-H. Ren, D. Qiu, C.-Y. Pang, Z. Li, Z.-G. Gu, Chem. Commun. 2015, 51, 788-791; e) D.-H. Ren, X.-L. Sun, L. Gu, D. Qiu, Z. Li, Z.-G. Gu, Inorg. Chem. Commun. 2015, 51, 50-54; f) L.-F. Qin, C.-Y. Pang, W.-K. Han, F.-L. Zhang, L. Tian, Z.-G. Gu, X. Ren, Z. Li, Dalton Trans. 2016, 45, 7340-7348; g) J. Ru, F. Yu, P.-P. Shi, C.-Q. Jiao, C.-H. Li, R.-G. Xiong, T. Liu, M. Kurmoo, J.-L. Zuo, Eur. J. Inorg. Chem. 2017, 2017, 3144-3149; h) K. E. Burrows, S. E. McGrath, R. Kulmaczewski, O. Cespedes, S. A. Barrett, M. A. Halcrow, Chem. Eur. J. 2017, 23, 9067-9075.

[13] a) I. y. A. Gural'skiy, V. A. Reshetnikov, A. Szebesczyk, E. Gumienna-Kontecka, A. I. Marynin, S. I. Shylin, V. Ksenofontov, I. O. Fritsky, J. Mater. Chem. C 2015, 3, 4737-4741; b) A. Naim, Y. Bouhadja, M. Cortijo, E. Duverger-Nédellec, H. D. Flack, E. Freysz, P. Guionneau, A. Iazzolino, A. Ould Hamouda, P. Rosa, O. Stefańczyk, Á. Valentín-Pérez, M. Zeggar, Inorg. Chem. 2018, 57, 14501-14512.

[14] a) Y. Sunatsuki, Y. Ikuta, N. Matsumoto, H. Ohta, M. Kojima, S. Iijima, S. Hayami, Y. Maeda, S. Kaizaki, F. Dahan, J.-P. Tuchagues, Angew. Chem., Int. Ed. 2003, 42, 1614-1618; b) D.-Y. Wu, O. Sato, Y. Einaga, C.-Y. Duan, Angew. Chem., Int. Ed. 2009, 48, 1475-1478; c) N. Hoshino, F. Iijima, G. N. Newton, N. Yoshida, T. Shiga, H. Nojiri, A. Nakao, R. Kumai, Y. Murakami, H. Oshio, Nat. Chem. 2012, 4, 921; d) S.-i. Ohkoshi, S. Takano, K. Imoto, M. Yoshikiyo, A. Namai, H. Tokoro, Nat. Photonics 2013, 8, 65-71; e) W. Liu, X. Bao, L.-L. Mao, J. Tucek, R. Zboril, J.-L. Liu, F.-S. Guo, Z.-P. Ni, M.-L. Tong, Chem. Commun. 2014, 50, 4059-4061; f) T. Romero-Morcillo, F. J. Valverde-Muñoz, M. C. Muñoz, J. M. Herrera, E. Colacio, J. A. Real, RSC Adv. 2015, 5, 69782-69789; g) I. y. A. Gural'skiy, O. I. Kucheriv, S. I. Shylin, V. Ksenofontov, R. A. Polunin, I. O. Fritsky, Chem. Eur. J. 2015, 21, 18076-18079; h) M. López-Jordà, M. Giménez-Marqués, C. Desplanches, G. Mínguez Espallargas, M. Clemente-León, E. Coronado, Eur. J. Inorg. Chem. 2016, 2016, 2187-2192; i) Y. Sekimoto, M. R. Karim, N. Saigo, R. Ohtani, M. Nakamura, S. Hayami, Eur. J. Inorg. Chem. 2017, 2017, 1049-1053.

[15] a) N. Bréfuel, S. Imatomi, H. Torigoe, H. Hagiwara, S. Shova, J.-F. Meunier, S. Bonhommeau, J.-P. Tuchagues, N. Matsumoto, Inorg. Chem. 2006, 45, 8126-8135; b) C. Bartual-Murgui, L. PiñeiroLópez, F. J. Valverde-Muñoz, M. C. Muñoz, M. Seredyuk, J. A. Real, Inorg. Chem. 2017, 56, 13535-13546.

[16] P. Gütlich, H. A. Goodwin, Spin Crossover in Transition Metal Compounds II, Vol. 234, Springer Berlin Heidelberg, Berlin, Heidelberg, 2004.

[17] P. Guionneau, M. Marchivie, Y. Garcia, J. A. K. Howard, D. Chasseau, Phys. Rev. B 2005, 72, 214408.

[18] a) Y. Garcia, P. Gütlich, in Spin Crossover in Transition Metal Compounds II, Springer Berlin Heidelberg, Berlin, Heidelberg, 2004, pp. 49-62; b) G. G. Morgan, K. D. Murnaghan, H. MüllerBunz, V. McKee, C. J. Harding, Angew. Chem., Int. Ed. 2006, 45, 7192-7195; c) C. Gandolfi, T. Cotting, P. N. Martinho, O. Sereda, A. Neels, G. G. Morgan, M. Albrecht, Dalton Trans. 2011, 40, 1855; d) B. Gildea, L. C. Gavin, C. A. Murray, H. Müller-Bunz, C. J. Harding, G. G. Morgan, Supramol. Chem. 2012, 24, 641-653; e) P. N. Martinho, B. Gildea, M. M. Harris, T. Lemma, A. D. Naik, H. Müller-Bunz, T. E. Keyes, Y. Garcia, G. G. Morgan, Angew. Chem., Int. Ed. 2012, 51, 12597-12601; f) K. Pandurangan, B. Gildea, C. Murray, C. J. Harding, H. Müller-Bunz, G. G. Morgan, Chem. Eur. J. 2012, 18, 2021-2029; g) B. Gildea, M. M. Harris, L. C. Gavin, C. A. Murray, Y. Ortin, H. Müller-Bunz, C. J. Harding, Y. Lan, A. K. Powell, G. G. Morgan, Inorg. chem. 2014, 53, 6022-6033; h) A. J. Fitzpatrick, E. Trzop, H. Müller-Bunz, M. M. Dîrtu, Y. Garcia, E. Collet, G. G. Morgan, Chem. Commun. 2015, 51, 17540-17543.

[19] a) M. Nakano, G.-e. Matsubayashi, T. Matsuo, in Adv. Quantum Chem., Vol. 44, Academic Press, 2003, pp. 617-630; b) S. Kimura, Y. Narumi, K. Kindo, M. Nakano, G.-e. Matsubayashi, Physical Review B 2005, 72, 064448; c) J. L. Her, Y. H. Matsuda, M. Nakano, Y. Niwa, Y. Inada, G. P., H. A., S. H., J. Appl. Phys. 2012, 111, 053921.

[20] C. Murray, B. Gildea, H. Müller-Bunz, C. J. Harding, G. G. Morgan, Dalton Trans. 2012, 41, 14487.

[21] C. R. Groom, I. J. Bruno, M. P. Lightfoot, S. C. Ward, Acta Crystallogr., Sect. B: Struct. Crystallogr. Cryst. Chem. 2016, 72, 171-179.

[22] a) K. Ishihara, M. Miyata, K. Hattori, T. Tada, H. Yamamoto, J. Am. Chem. Soc. 1994, 116, 10520-10524; b) M. Periasamy, L. Venkatraman, S. Sivakumar, N. Sampathkumar, C. R. Ramanathan, J. Org. Chem. 1999, 64, 7643-7645; c) M. Periasamy, C. Ramaraj Ramanathan, N. S. Kumar, Tetrahedron: Asymmetry 1999, 10, 2307-2310; d) M. Periasamy, N. S. Kumar, S. Sivakumar, V. D. Rao, C. R. Ramanathan, L. Venkatraman, J. Org. Chem. 2001, 66, 3828-3833; e) T. Tu, T. Maris, J. D. Wuest, Cryst. Growth Des. 2008, 8, 1541-1546.

[23] C. Carter, S. Fletcher, A. Nelson, Tetrahedron: Asymmetry 2003, 14, 1995-2004.

[24] A. Spek, Acta Crystallogr., Sect. C: Struct. Chem. 2015, 71, 9-18.

[25] S. Alvarez, D. Avnir, M. Llunell, M. Pinsky, New J. Chem. 2002, 26, 996-1009.

[26] M. G. B. Drew, C. J. Harding, V. McKee, G. G. Morgan, J. Nelson, Chem. Commun. 1995, 1035-1038.

[27] S. Mauskopf, in Chiral Analysis, Elsevier, Amsterdam, 2006, pp. 3-24.

[28] C. E. Housecroft, A. G. Sharpe, Inorganic Chemistry, 2012.

[29] O. Kahn, Molecular magnetism, VCH, 1993.

[30] Y. Garcia, O. Kahn, J.-P. Ader, A. Buzdin, Y. Meurdesoif, M. Guillot, Phys. Lett. A 2000, 271, 145-154.

[31] R. C. Clark, J. S. Reid, Acta Crystallogr., Sect. A: Cryst. Phys., Diffr., Theor. Gen. Crystallogr. 1995, 51, 887-897.
[32] G. Sheldrick, Acta Crystallogr., Sect. A: Cryst. Phys., Diffr., Theor. Gen. Crystallogr. 2015, 71, 3-8.
[33] G. Sheldrick, Acta Crystallogr., Sect. C: Struct. Chem. 2015, 71, 3-8.